ACS APPLIED MATERIALS & INTERFACES

Research Article

www.acsami.org

Robust and Flexible Fabrication of Chemical Micropatterns for Tumor Spheroid Preparation

Tianqing Liu, Chih-Tsung Yang, Lorena Dieguez, John A. Denman, and Benjamin Thierry*

Ian Wark Research Institute, University of South Australia, Mawson Lakes Campus, Mawson Lakes, Adelaide, South Australia 5095, Australia

Supporting Information

ABSTRACT: A robust and flexible approach is described for the straightforward preparation of multicellular tumor spheroids of controllable dimensions. The approach is based on a one-step plasma polymerization of the monomer allylamine carried out through conformal micropatterning physical masks that is used to deposit amine-rich (PolyAA) micrometer-scale features that promote cellular attachment and initiate the formation of multicellular spheroids. A simple backfilling step of the nonpolymerized poly(dimethylsiloxane) background with Pluronic F127 significantly reduced background cellular adhesion on the untreated substrate and, in turn, improved the quality of the spheroid formed. Tumor cells grown on the PolyAA/F127 patterned surfaces reliably formed multicellular spheroids within 24−48 h depending on the cell type. The dimension of the spheroids could be readily controlled by the dimension of the amine-rich micropatterns. This simple approach is compatible with the long-term culture of multicellular spheroids and their characterization with high-resolution optical microscopy. These features facilitate the development of on-chip assays, as demonstrated here for the study of the binding of transferrin-functionalized gold nanoparticles to multicellular tumor spheroids.

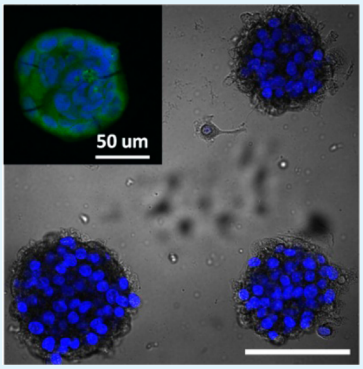

KEYWORDS: *multicellular tumor spheroids, micropatterning, plasma polymers, gold nanoparticles, immunotargeting*

1. INTRODUCTION

Cancer research has historically relied on a 2D culture of cancer cell lines for in vitro studies. It is, however, now well-established that such 2D culture systems lack many of the key features of tumor tissues and, consequently, are only poor mimics with limited relevance to the in vivo situation. On the other hand, multicellular 3D tumor models have been shown to better represent the complexity and pathophysiology of tumor tissues.[1,2] Therefore, cellular 3D tumor models are of very high interest in cancer research, for instance, toward elucidating fundamental aspects of tumor cell biology or for anticancer drug screening.[3−7]

Despite its merits, the most established method to prepare tumor spheroids, the hanging-drop method, remains inherently limited in its abilities in forming large numbers of uniform spheroids, which is a key requirement toward standardizing biological studies and toxicity or efficacy measurements. However, a notable advancement has been the development of a 384-format hanging-drop array plate as a user-friendly solution to spheroid formation and culture.[8] Taking advantage of microfabrication advancements, new approaches have been applied to 3D tumor tissue engineering in order to form high-quality tumor spheroids in a more controlled fashion.[9] One efficient approach relies on the fabrication of arrays of microwells with dimensions in the hundreds of micrometers. Microwells provide a confined environment for the tumor cells, enhancing cell−cell interactions and, consequently, fostering the formation of 3D cell aggregates within the microwells.[10] The main drawbacks associated with microwell-based approaches are the need for microfabrication facilities, the lack of compatibility with high-resolution imaging techniques, and the occasional presence of multiple spheroids in a single well.[11] In addition, multicellular spheroids grown in microwells are easily displaced during media changes. While this feature can be advantageous in some applications that require ex situ processing of the spheroids, the associated risk of loss of tumor microtissues is a challenge for long-term "on-chip" culture and often precludes the design of quantitative integrated assays. The integration within microfluidics of microwell−spheroid formation approaches is, however, offering promising opportunities to design advanced on-chip assays.[12,13]

Perhaps the easiest approach to enhancing cell−cell interactions and generating tumor spheroids is the use of surfaces resistant to cellular binding. Many approaches can be used to prepare such nonbinding surfaces, for instance, through the use of poly(2-hydroxyethyl methacrylate) (poly-HEMA) and poly(ethylene glycol) coatings. The main limitation of this general strategy is the lack of control over the dimensions of the spheroids.[11] Of particular interest, in view of their simplicity and versatility, are methods based on the fabrication of cell-adhesive micropatterns on a nonadhesive background. Cell-adhesive patterns act as nucleation points for cell aggregation,

Received: March 11, 2014
Accepted: June 4, 2014
Published: June 4, 2014

leading to the formation of spheroids with good control over the dimensions.[14−19] The prepared spheroids can be readily imaged using light microscopy, at least when prepared on glass substrates, and can be grown for a long period of time using gentle media changes.

Cell-adhesive chemical patterns (i.e., binding/nonbinding contrasts) can be prepared using a number of methods, including microcontact printing,[20] inkjet printing,[21] covalent bonding reactions with spatially chemically functionalized surfaces,[22] preparation of binding/nonbinding substrates using selective plasma dry etching or ion implantation,[23,24] and cell-transfer printing.[25] A simple and direct method to modify surfaces for biological applications is plasma micropatterning.[26,27] Plasma polymerization reliably produces thin conformal coatings with a broad range of chemistries relevant to the control of cellular adhesion. Of particular interest are amine-rich plasma-polymerized coatings that significantly enhance cell adhesion.[1,28−33] The thickness of plasma polymer layers can be easily controlled, and uniform layers can be prepared over large surface areas. Plasma-based surface methods for cell patterning can be divided into plasma etching,[23] plasma wetting-controlled deposition patterning,[34] and grafting of nonfouling polymer films and/or fouling polymeric films.[35−37] These methods rely on the use of multiple plasma processes to prepare cell-adhesive and nonadhesive areas on the substrate or upon removal of photolithographic patterned regions to create cell-binding patterns. An alternative and straightforward one-step method to create plasma polymer patterns is the use of conformal physical masks.[38]

Toward establishing a simple yet reliable approach to prepare high-quality tumor spheroids compatible with high-resolution microscopy and long-term culture for on-chip biological assays, we report here a method to create cell-adhesive patterns over a cytophobic background. The method is based on the plasma polymerization of amine-rich thin films through poly(dimethylsiloxane) (PDMS) physical masks on glass coverslips coated with a thin PDMS layer (Scheme 1). The PDMS layer enables a high level of conformality of the PDMS physical micropatterning masks during the plasma polymerization step. In addition, a single step of backfilling of the nonplasma-polymerized PDMS surface with Pluronic F127 minimizes cellular binding. To demonstrate the utility of this approach and its compatibility with molecular studies, tumor spheroids formed on the PolyAA/F127 micropatterned coverslips were used to study the binding of cancer-targeted gold nanoparticles. To this end, gold nanoparticles were biofunctionalized with transferrin and their binding to the spheroids imaged using a VivaScope reflectance confocal system.

2. EXPERIMENTAL SECTION

Fabrication of PDMS Micropatterning Physical Masks Using Photolithography. PDMS micropatterning physical masks with various diameters of the pattern size were fabricated using photolithography and a dry lift-off strategy.[39] Briefly, the design contains arrays of circular holes with diameters ranging from 80 to 500 μm. Edge-to-edge spacing between the patterns ranged from 100 to 250 μm. The negative photoresist SU-8 50 (Microchem Corp.) layer (100−200 μm thickness) was spun on glass slides at controlled speeds. After soft baking on a hot plate at 65 °C for 2 min, UV exposure through the photomasks was applied at 400−450 mJ/cm^2. Postexposure baking was carried out at 65 °C for 2 min followed by 95 °C for 10 min. The samples were then developed and cleaned using isopropyl alcohol. The developed SU-8 was hard baked at 65 °C for 2 min and then 95 °C and left to cool to room temperature. SU-8 masters were then hydrophobized using trichloroperfluorooctylsilane (0.1 mM) to create a nonsticking layer and facilitate release of the PDMS physical masks. PDMS (Sylgard 184, Dow Corning, USA) was prepared by mixing the elastomer and curing agent with a ratio of 10:1 (w/w). A thin layer of the mixture was quickly spun over the SU-8 masters to achieve thicknesses of 30−50 μm, making sure that the thickness of the PDMS layer is lower than that of the SU-8 features. After curing and cooling, PDMS masks could be gently peeled off from the SU-8 master.

Scheme 1. Preparation of the Micropatterned Microarray and Multicellular Tumour Spheroid Formation on the Patterned Surfaces

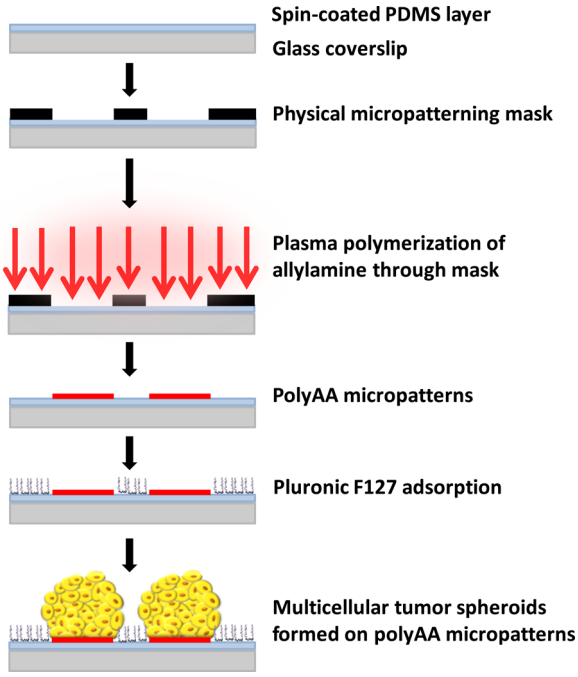

Chemical Micropatterning Using Plasma Polymerization. First, a glass coverslip was homogeneously coated with a thin spin-coated layer of PDMS (~30−50 μm) and cured at 65 °C for 2 h. The thickness of the PDMS layer was confirmed by a Filmetrics F20 optical spectrometer (Filmetrics, USA). A PDMS micropatterning physical mask was then placed carefully on top of the PDMS-coated coverslip (Scheme 1). The amine-rich cell-adhesive features were then deposited through the micropatterning physical masks using plasma polymerization of the monomer allylamine (Sigma-Aldrich, USA) using a custom-built reactor reported previously.[38,40] Briefly, the reactor chamber is defined by a glass cylinder with a height of 35 cm and a diameter of 17 cm. The gas pressure is monitored via a Pirani gauge and controlled by needle valves (BOC Edwards). The typical base pressure prior to the introduction of the monomer was 0.03 mbar. A monomer pressure of 0.20 mbar and a treatment time of 1 min were used. The micropatterning physical mask is then carefully removed from the coverslips. The process resulted in the deposition of amine-rich plasma-polymerized thin patterns (PolyAA) on the PDMS-coated coverslips.

Next, to minimize nonspecific cellular binding of the PDMS background nontreated with PolyAA, the whole coverslip surface was incubated with Pluronic F127 (1 wt %) for 12 h. The samples were finally washed with Milli-Q water, sterilized with 70% ethanol, and kept in a sterilie environment prior to use.

Surface Analysis of the Micropatterns. X-ray photoelectron spectroscopy (XPS) analyses were conducted using a Kratos AXIS Ultra DLD XPS spectrometer with a monochromatic Al Kα X-ray source ($h\nu$ = 1486.69 eV) and a hemispherical analyzer. The pass energy was 20 eV with a resolution of 0.3 eV for high-resolution

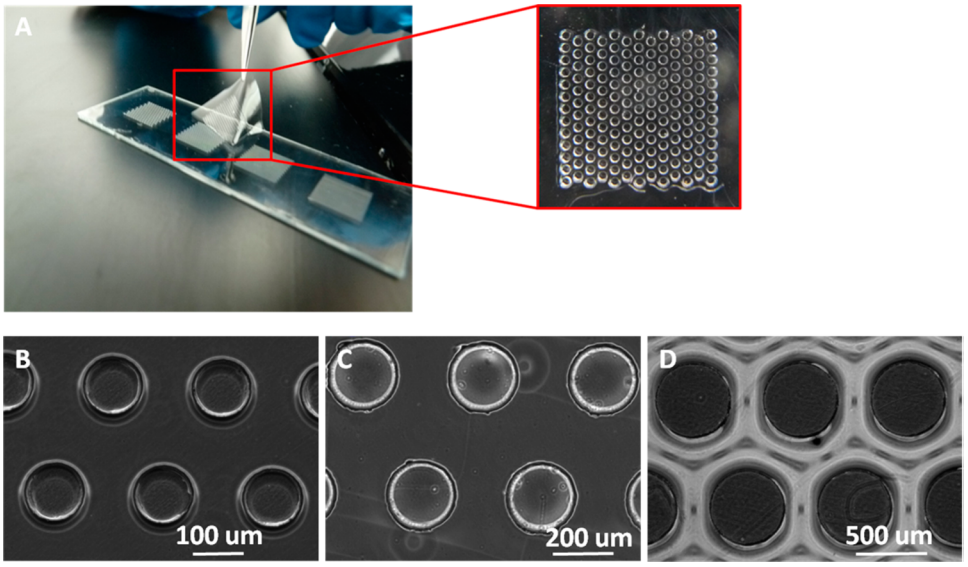

Figure 1. Fabrication of PDMS micropatterning physical masks using photolithography: (A) dry lift-off of a membrane; microscopic images of PDMS physical micropatterning masks with pattern diameters of (B) 100, (C) 200, and (D) 500 μm.

spectra. Spectra were collected at a photoelectron takeoff angle of 90°. Binding energies were referenced to the C 1s hydrocarbon peak at 285.0 eV to compensate for surface charging effects. Component fitting of high-resolution spectra was performed using *CasaXPS*, version 2.3.12, software. Shirley-type backgrounds were used and components constrained to full width at half-maximum between 0.9 and 1.5 eV. The peak fits used 70% Gaussian/30% Lorentzian peak shapes.

Time-of-flight secondary-ion mass spectrometry (TOF-SIMS) analyses were conducted using a Physical Electronics Inc. PHI TRIFT V nano-TOF instrument (Physical Electronics, Inc., Chanhassen, MN) equipped with a pulsed liquid metal $^{79+}$Au primary ion gun, operating at 30 kV energy. Dual-charge neutralization was provided by an electron flood gun (10 eV electrons) and 10 eV Ar^+ ions. Experiments were performed under a vacuum of 5×10^{-6} Pa or better. "Bunched" Au_1 instrumental settings were used to optimize spectral resolution for the collection of positiv-mode SIMS spectra. Sample spectra were processed and interrogated using *WincadenceN* software (version 1.11.2). Principal component analysis (PCA) was conducted with *STATISTICA* software (version 7.0) using a covariance matrix.

Cell Culture and Cell Adhesion Experiments on the Surfaces. The mammary carcinoma cell line EMT-6 was cultured in T-25 flasks in Dulbecco's modified Eagle medium (DMEM)/F12 supplemented with 10% fetal bovine serum, penicillin (100 U/mL), and streptomycin (0.1 mg/mL) at 37 °C in a humidified incubator at 37 °C, 5% CO_2, and 100% humidity. The human breast cancer cell line MCF-7 (ATCC, USA) was grown in complete media consisting of DMEM supplemented with 10% (v/v) fetal bovine serum. Small flat pieces of PDMS were cut and coated uniformly with either the amine-rich PolyAA or Pluronic F127, as described in the previous section. Cells (100 μL, 1×10^5 cells/mL) were seeded and allowed to attach on the samples for 8 h in a humidified incubator at 37 °C, 5% CO_2, and 100% humidity. After gentle washing, the cells attached on the samples were imaged using an inverted light microscope (Nikon Eclipse TE, Japan) and counted in 10 randomly chosen fields of view.

Formation of the Tumor Spheroid Arrays. The PolyAA/F127 micropatterned coverslips were mounted onto custom-made PDMS wells (typically 1 cm in diameter). The samples were first equilibrated with a cell culture medium 30 min before cell seeding. Cell suspensions (200 μL, 1×10^6 cells/mL) were then seeded onto the samples. The culture medium was removed every 2 days and refilled with a fresh medium. The samples were cultured in an incubator at 37 °C, 5% CO_2, and 100% humidity for up to 14 days. Cells grown on PDMS-coated glass coverslips treated with either adhesive plasma polymers or Pluronic F127 were used as controls.

Aggregation of the cells and formation of the tumor spheroids on the adhesive patterns were monitored using an inverted light microscope (Nikon Eclipse TE, Japan). Next, the formed multicellular tumor spheroids were fixed in cold methanol and stained with 4′,6-diamidino-2-phenylindole (DAPI) for 5 min in the dark at room temperature. The spheroids were imaged using confocal microscopy (LSM710, Zeiss). A coarse scan of the z-stacks of EMT-6 multicellular tumor spheroids prepared on 100 μm micropatterned arrays was carried out to obtain the 3D structure of the spheroids. Spheroids were also stained with Rhodamine Phalloidin (50 μg/mL) at room temperature for 30 min to visualize the F-actin of the cells. Cells were washed with phosphate-buffered saline (PBS) before being imaged by confocal microscopy.

Gold Nanoparticle Synthesis and Biofunctionalization with Transferrin. Gold nanoparticles were synthesized and biofunctionalized as reported previously.[41,42] Briefly, a $HAuCl_4$ solution (1 wt %) was boiled with a sodium citrate solution (1 wt %) for 10 min to synthesize gold nanoparticle seeds (approximately 20 nm). The seeds were then grown into 100 nm nanoparticles by reducing $HAuCl_4$ using a 1% citrate solution (22 μL) and a 0.03 M hydroquinone solution (100 μL). The synthesized gold nanoparticles were treated with a small amount of 0.05% (v/v) Tween 20 for 30 min to increase the shelf life of the nanoparticles. After purification of the gold nanoparticles, PEGylation was carried out with a 4:1 molar mixture of MW 5000 PEG (Rapp Polymer Gmbh) and 458 PEG (Polypure) solutions under vortexing and left to react for at least 6 h. The PEGylated nanoparticles were activated by NHS/EDC for 5 min and incubated with a human transferrin solution (50 μg/mL in PBS). The transferrin-conjugated gold nanoparticles were washed with PBS to remove excess transferrin and kept at 4 °C prior to use. As-synthesized gold nanoparticles prepared on a copper grid were analyzed using a Philips CM100 transmission electron microscope. UV−vis spectra were determined using a Varian Cary 5 UV−vis−near-IR spectrophotometer at room temperature.

Cellular Uptake of the Transferrin-Functionalized Gold Nanoparticles. To confirm the specific targeting of transferrin-functionalized gold nanoparticles, an in vitro cellular uptake study was carried out using MCF-7 human breast cancer cells. Cells were seeded onto poly(D-lysine)-coated glass coverslips for 24 h, washed with a fresh DMEM medium, and incubated for 2 h at 37 °C with gold nanoparticles conjugated with either human transferrin or PEGylated gold nanoparticles used as a control (gold concentration of 0.04 mM). Cells were then extensively washed with PBS, fixed in a formalin

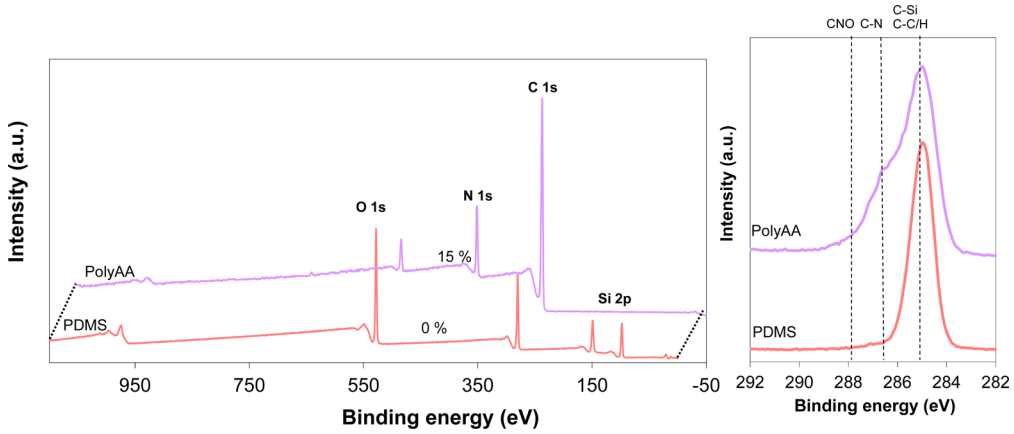

Figure 2. XPS survey spectra and C 1s high-resolution spectra of a PolyAA plasma film deposited on PDMS. The dashed lines show binding energies of carbon atoms in C−Si/C−H (285 eV), C−O/C−N, (286.5 eV), and −C═O/N−C═O (288 eV) environments.

solution (10% formaldehyde) at room temperature for 10 min, and then washed again (2 × 1 mL). The cellular uptake of the nanoparticles was visualized using a reflectance confocal microscope (LSM510, Zeiss) as described previously.[41,42]

Gold Nanoparticle Targeting to Micropatterned Tumor Spheroids. MCF-7 multicellular tumor spheroid arrays prepared on the PolyAA/F127 patterned coverslips were treated with PEGylated and transferrin-conjugated gold nanoparticles at a gold concentration of 0.04 mM for 12 h in a tissue culture incubator. After incubation, the spheroids were washed thoroughly with PBS (3 × 1 mL) to remove unbound nanoparticles. The spheroids were then fixed in a formalin solution (4% formaldehyde) at room temperature for 6 h and washed (2 × 1 mL) with PBS. The binding of the targeted and nontargeted gold nanoparticles in the spheroids was imaged with a VivaScope 1500 multilaser reflectance confocal microscope (Caliber Imaging & Diagnostics, Rochester, NY). The reflectance images were acquired using a 658 nm laser source at a power of 4.0 mW.

3. RESULTS AND DISCUSSION

Fabrication of PDMS Micropatterning Physical Masks. The characteristics of the PDMS micropatterning physical masks were controlled during photolithography of the SU-8 masters. Dimensions relevant to the formation of multicellular tumor spheroids were chosen for micropatterning of the PolyAA cell-adhesive areas. Silane-based hydrophobization of the SU-8 master enabled easy release of the PDMS physical masks without damaging the SU-8 features or the membrane masks (Figure 1A). Typically, the micropatterning masks were fabricated with thicknesses in the range of 30−50 μm. Optical microscopic images of the masks confirmed the presence of well-defined physical patterns (Figure 1B−D).

Preparation and Characterization of PolyAA Cell Adhesive on PDMS Layers. The surface chemistry of the plasma-polymerized allylamine cell-adhesive layer was characterized by XPS. Elemental XPS analysis showed the appearance of a peak at ∼400 eV, which is associated with nitrogen (N 1s) and was not present in the spectrum of the unmodified PDMS, confirming the successful deposition of the allylamine plasma-polymerized layer enriched in nitrogen (15% of the elemental composition). The Si 2p peak characteristics of siloxane were not detectable after plasma polymerization of the allylamine monomer, confirming deposition of a homogeneous plasma polymer film. Analyses of the XPS C 1s core-level spectra were then carried out to ascertain the surface chemistry. Three components were necessary to component fit the C 1s core-level spectra (Figure 2) of the PolyAA samples. The first component, located at 285.0 eV, was attributed to hydrocarbon and C−Si. The second component at 286.5 eV was attributed to carbon singly bonded to nitrogen or oxygen. The third component at 288.1 eV was attributed to carbon atoms in amide groups (N−C═O) as well as in carbonyl compatible with the presence of oxygen in the PolyAA layer.

Next, TOF-SIMS was used to investigate the interactions between F127 and the PDMS and PolyAA surfaces. PCA of the TOF-SIMS data was conducted, and the score and loading plots are presented in Figure 3. The score plot shows distinct clustering of each surface, indicating significantly different chemistries for each. The greatest variation between the surfaces is represented in the first principal component (∼77%), which is negatively correlated to those surfaces that have undergone PolyAA plasma polymerization treatment. The second principal component (∼22%) highlights the additional F127 treatment, which from the loading plot can be seen to correlate with the expected $C_xH_yO_z$ peak fragment chemistry. From PCA of the TOF-SIMS data, it can therefore be concluded that F127 adsorbs on the PolyAA surfaces. Importantly, previous studies have demonstrated that physically adsorbed Pluronic displays different conformations, depending on the hydrophobicity of the substrate. While Pluronic copolymers adopt brushlike conformations on hydrophobic surfaces (water contact angle above ∼80°), which result in high fouling resistance, the terminal PEO_n [PEO = poly(ethylene oxide)] blocks interact strongly with the hydrophilic surfaces, which result in the adoption of pancake conformations.[43,44] Pluronic adsorbed onto hydrophilic surfaces has therefore low fouling resistance in comparison to Pluronic adsorbed onto hydrophobic substrates. This characteristic is used here to ensure that cellular adhesion onto the PolyAA patterns is not compromised even after exposure to the Pluronic passivation layer.

Cell Binding on the PolyAA Surface versus Pluronic F127-Treated PDMS. In order to investigate cell behaviors on the treated surfaces, in vitro cell culture was performed on the cell-adhesive PolyAA-coated PDMS and cell-resistant Pluronic F127-coated PDMS. A contact time of 8 h was used to enable the cells to bind to the surfaces. Clear differences in the binding of cancer cells as well as in their morphologies were observed (Figure 4). Cell densities on the PolyAA surface were high, and most cells were extensively spread, suggesting strong cell−substrate adhesion on the amine-rich surface prepared by plasma polymerization. The cell-binding enhancement proper-

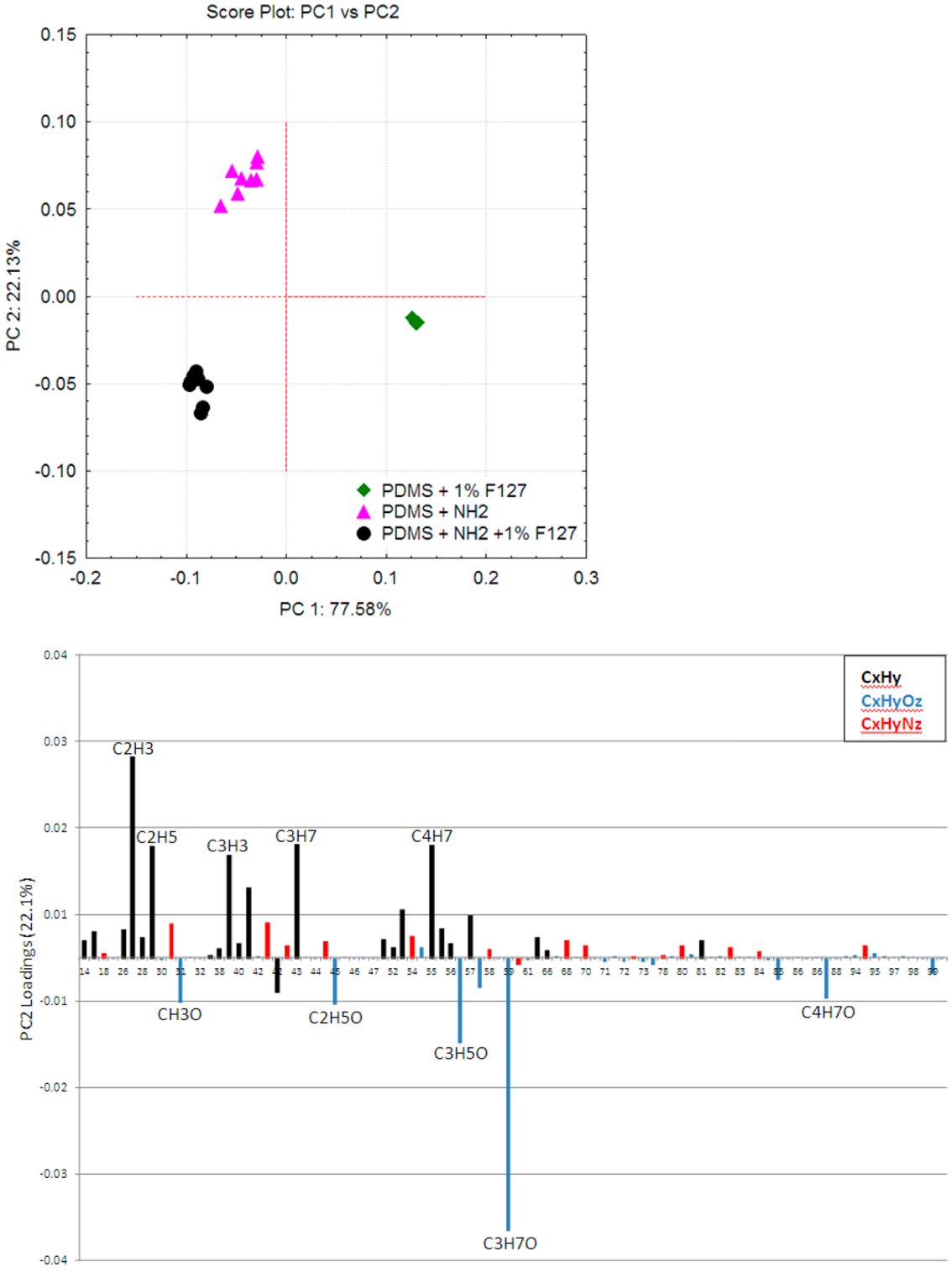

Figure 3. PCA score and loading plots for TOF-SIMS data for PDMS treated with 1% F127, PolyAA (PDMS + NH_2), and PolyAA treated with 1% F127 (PDMS + NH_2 + 1% F127).

ties of amine functional groups on solid substrates have been well demonstrated using a broad range of cell lines, such as rat cerebellar granule neurons,[45] human embryonic kidney cells,[46] osteoblasts,[30] human skin fibroblast,[29] and human endothelial cells.[28] On the other hand, much fewer cells attached and spread on the Pluronic F127-treated PDMS surface (118 ± 30 cells/mm^2) compared with the PolyAA-modified surfaces (1314 ± 93 cells/mm^2) as well as the untreated PDMS (444 ± 87 cells/mm^2) (Figure 4A–D). These results are in agreement with previously reported studies that demonstrated that Pluronic F127-coated PDMS can resist cell attachment because of the cell-repelling nature of the hydrophilic PEO side chains.[34,47,48] Altogether, this study confirmed the suitability of the chosen chemical design toward the formation of tumor spheroids with controllable dimensions.

dx.doi.org/10.1021/am501390v | ACS Appl. Mater. Interfaces 2014, 6, 10162–10171

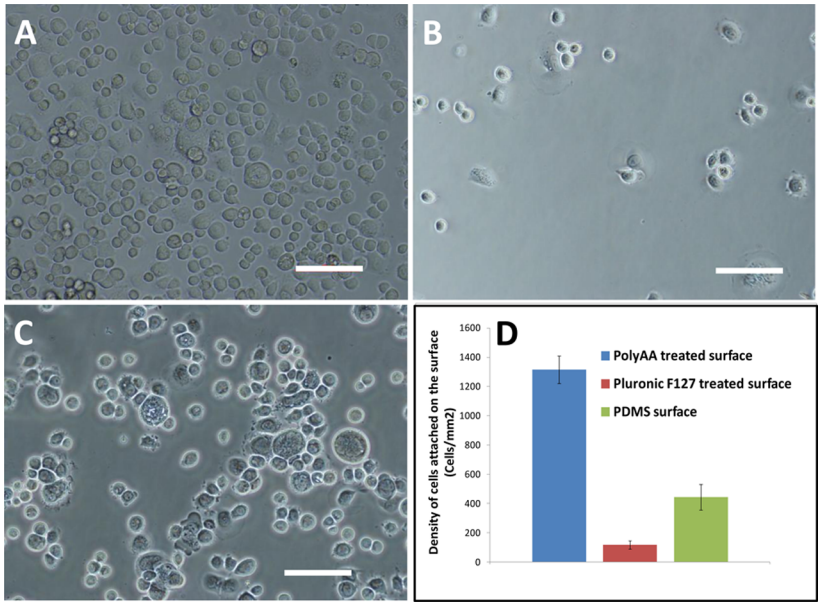

Figure 4. MCF-7 cell attachment on functionalized PDMS surfaces after 8 h of cell culture: (A) PolyAA-coated PDMS; (B) Pluronic F127-treated PDMS; (C) untreated PDMS. Scale bars are 100 μm. (D) Densities of cells attached on the PolyAA-coated PDMS, Pluronic F127-treated PDMS, and untreated PDMS surfaces at the 8 h time point.

Spheroid Formation on Micropatterned Surfaces. Next, arrays of cell-adhesive PolyAA features were created on the surface of PDMS-coated coverslips using the conformal micropatterning physical masks. After the polymerization process, the micropatterning masks were carefully removed from the coverslips, leaving the PolyAA features intact. The samples were then washed and incubated with F127 for 12 h. Finally, the samples were thoroughly rinsed with water and immersed in 70% ethanol prior to cell culture. Scheme 1 summarizes the successive steps of the process. The formation of tumor spheroids could be monitored continually over time by mounting the samples within a stage top incubator. After MCF-7 tumor cells were seeded onto the binding/nonbinding micropatterned surfaces using custom-made macrowells, cells began to attach within 1 h onto the PolyAA adhesive patterns and gradually spread over the next few hours. This finding confirmed that the adsorption of Pluronic molecules onto the PolyAA surface, as detected by TOF-SIMS, did not compromise the cytocompatibility of the NH_2-rich plasma-polymerized surfaces. On the other hand, only small numbers of cells adhered to the F127-coated regions. 3D spheroids formed on the surface after 48 h and continually grew over the course of the experiments (Figure S1 in the Supporting Information). As shown in Figure 5, the dimensions of the spheroids were precisely defined by the dimensions of the cell-adhesive PolyAA micropatterns, which enabled the formation of spheroids with diameters of approximately 100, 200, and 500 μm. No spheroid detachment or disassembly was observed from the micropatterned arrays during the experiments, even for long-term cell culture (>14 days). This is an advantageous feature of the adhesive micropattern approach because loss of tumor microtissues during media manipulation that are inherently required to carry out drug assays compromises the design of quantitative studies. On the other hand, detachment of multicellular spheroids in response to exposure to cytotoxic drugs, for instance, could occur, necessitating careful manipulation at the final stage of the assays. Importantly, the spheroids could be easily dissociated to recover a single cell

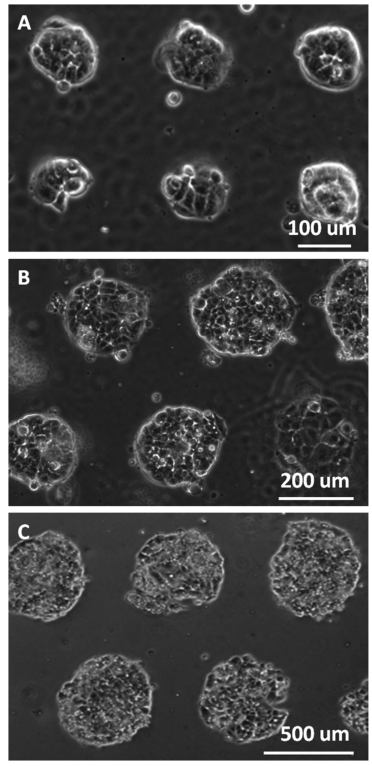

Figure 5. Phase contrast images of MCF-7 multicellular tumor spheroids cultured for 14 days using (A) 100, (B) 200, and (C) 500 μm micropatterning masks.

suspension for further analysis. EMT-6 cell spheroids could also be easily prepared on the micropatterned surfaces and formed as early as after 24 h of culture, showing continuous growth for 7 days and demonstrating the versatility of the proposed approach.

Next, high-resolution images of the spheroids were obtained using confocal microscopy. Cell nuclei stained with DAPI were

imaged and combined with differential interference contrast (DIC) to characterize the cell distribution within the multicellular spheroids, confirming that high-resolution images can be easily obtained using the proposed simple and robust micropatterning approach (Figure 6A,B). Z-stack images of the cell nuclei of the patterned spheroids were reconstructed to obtain 3D spheroids (Figure 6C). The thicknesses of the spheroids matched the diameters of the cell-adhesive patterns. For instance, for spheroids prepared on the 100 μm patterns, the thickness of the microtissues ranged from 85 to 110 μm, as estimated by confocal microscopy. Cells distributed homogeneously within the spheroids. Figure 6D showed the formation of an actin filament within the MCF-7 spheroids, confirming the high level of cell−cell interactions, which is a key requirement to mimic in vivo tumor tissues. Altogether, these results confirmed that uniform and well-organized multicellular tumor spheroids are formed on the PolyAA cell-adhesive patterns. Plasma polymerization through physical masks is a very robust and flexible methodology that enables the formation of adherent, pinhole-free, and conformal coatings with a broad range of shapes and dimensions. In addition, plasma processes are easily up-scalable and highly reproducible and can be applied to a broad range of substrates. The proposed patterning process could be, for instance, applied to standard tissue-culture well-plates, taking advantage of the good physical adsorption of Pluronic on polystyrene. These features make the proposed approach a promising alternative to the micropatterning-based spheroid formation methodologies previously reported.[12−19]

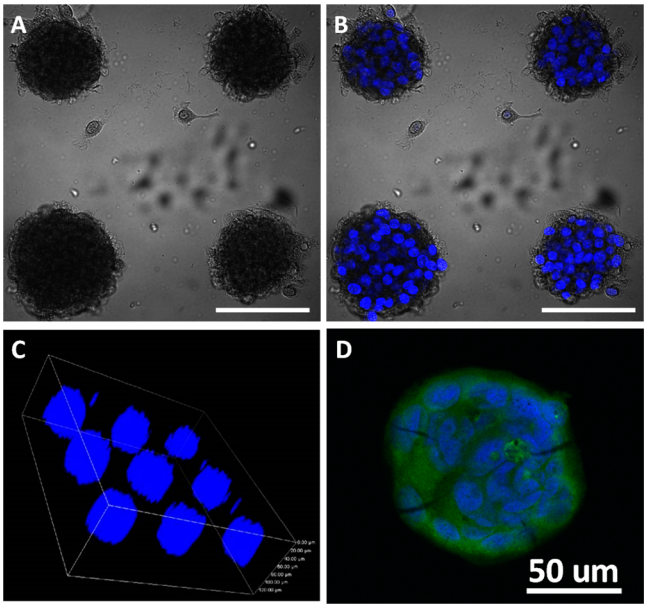

Figure 6. DIC (A) and fluorescence (B) microscopic imaging of EMT-6 multicellular tumor spheroids prepared on 100 μm micropatterned arrays using confocal microscopy. (C) 3D reconstruction of the EMT-6 multicellular spheroids prepared on 100 μm micropatterned arrays displaying the 3D structure of the microtissues. Cell nuclei have been stained with DAPI (scale bars are 100 μm; the Z scale of part C is 120 μm). (D) Fluorescence imaging of EMT-6 multicellular spheroids stained with DAPI and Rhodamine Phalloidin.

Targeting of Transferrin-Conjugated Gold Nanoparticles to Tumor Spheroids. Understanding the binding of nanoparticles inside tumor tissues is of high importance, and the utility of the spheroids formed using the proposed plasma micropatterning approach was demonstrated here in a feasibility study to investigate the binding of transferrin-conjugated gold nanoparticles. Gold nanoparticles larger than 60 nm have an inherently high scattering and, consequently, enable direct visualization of cellular binding with light microscopy, for instance, reflectance confocal microscopy.[49,50] Gold nanoparticles with diameters of 100 nm were therefore

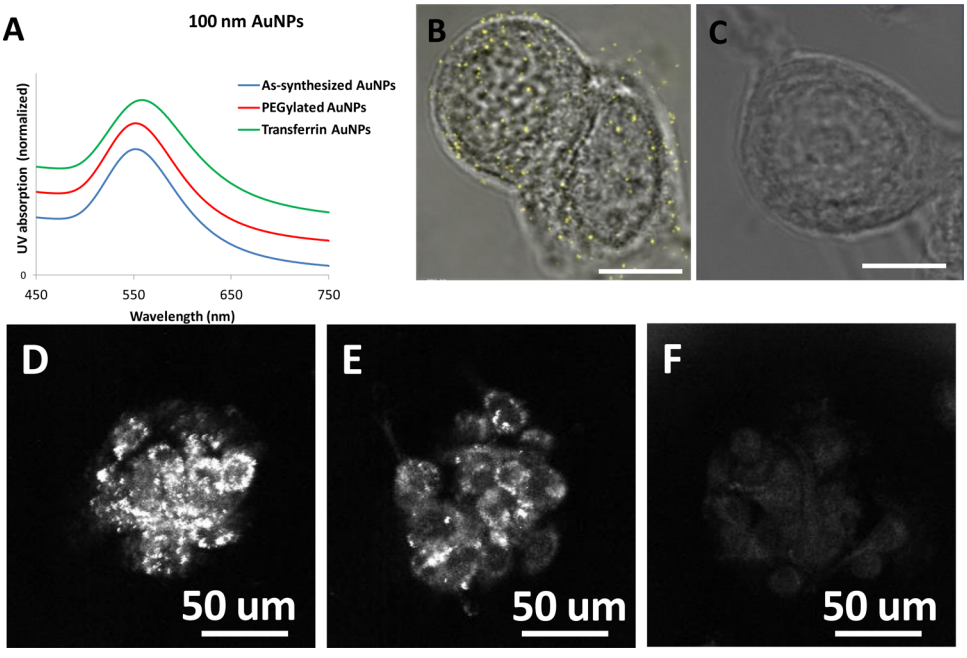

Figure 7. (A) UV−vis absorption of the as-synthesized, PEGylated, and transferrin-conjugated gold nanoparticles (AuNPs). Reflectance confocal microscopic images (bright field, reflectance, and overlay) of (B) transferrin AuNPs and (C) PEGylated AuNPs binding to MCF-7 cells (scale bars are 10 μm). Vivascope reflectance confocal microscopy of 100 μm MCF-7 multicellular spheroids treated for 12 h with (D) transferrin AuNPs, (E) PEGylated AuNPs, and (F) control (no AuNPs) (scale bars are 50 μm).

used in this study. PEGylation of the gold nanoparticles was carried out using an optimized protocol designed to increase the nanoparticle stability and bioconjugation yields.[41,42] Human holotransferrin is a well-established ligand for cancer cell targeting and shows high binding affinity to MCF-7 cells.[51,52] Transferrin conjugation with gold nanoparticles was achieved by coupling the carboxylic moieties on the optimized PEG coating with primary amines on human transferrin via carbodiimide chemistry. UV−vis absorption of the gold nanoparticles before and after bioconjugation confirmed the good stability and successful surface modification (Figure 7A), which is in agreement with our previously published reports.[41,42] The in vitro cellular uptake of the transferrin-conjugated gold nanoparticles to the human cancer cell line MCF-7 was studied by reflectance confocal microscopic imaging. Significantly higher binding of the transferrin gold nanoparticles was observed in the reflectance images (Figure 7B) in comparison to the control PEGylated gold nanoparticles (Figure 7C). These results demonstrate the high binding affinity and specificity of the transferrin-conjugated nanoparticles at the single-cell level.

Next, the binding of transferrin gold nanoparticles to MCF-7 spheroid was investigated. The optical contrast resulting from the binding of gold nanoparticles in MCF-7 tumor spheroids was visualized using a VivaScope 1500 Multilaser reflectance confocal microscope, which is a clinically used reflectance imaging system. Parts D−F of Figure 6 show that the gold nanoparticles bound to the tumor spheroids could be observed as bright spots in the reflectance images. Higher levels of reflectance contrast for the spheroids treated with transferrin-conjugated nanoparticles were observed, demonstrating that transferrin-enabled active targeting to the MCF-7 cells occurs throughout the whole spheroid. On the other hand, non-conjugated PEGylated nanoparticles showed significantly lower binding and uptake by the cancer cells within the spheroids (Figure 7E). Although low in comparison to their targeted counterpart, the presence of nontargeted nanoparticles in the spheroids suggests that complex interaction takes place within the microtissues that cannot be readily predicted from 2D cell layers. While only small spheroids (diameter of 100 μm) were used in this feasibility study, these data confirmed the possibility of using the plasma-micropatterned approach to study the uptake of nanoparticles inside tumor spheroids. Considering the growing importance of immunotargeted cancer nanomedicine agents, a systematic study of their binding kinetics, transport, and clearance inside tumor tissues is required, and the proposed micropatterned spheroid formation approach is ideally suited to provide these important mechanistic insights.

4. CONCLUSION

Cell-binding/nonbinding micropatterned surfaces have been prepared using a simple one-step method based on plasma polymerization of the allylamine monomer through conformal micropatterning physical masks and backfilling of the untreated region with Pluronic F127. The micropatterned substrates could be readily used to form multicellular 3D tumor spheroids of controllable dimensions. The proposed approach enables easy long-term on-chip culture of the spheroids and is compatible with high-resolution light microscopy. Importantly, the attachment of the spheroids to the micropatterned surface prevents the loss of tumor microtissues during media manipulation, which is a useful feature toward the design of quantitative spheroid-based assays. It is envisaged that this approach will facilitate the use of multicellular spheroids in cancer research and a feasibility study is carried out here where the plasma-micropatterned approach is used to study the binding of transferrin-conjugated gold nanoparticles to tumor spheroids.

■ ASSOCIATED CONTENT

Supporting Information

Time-lapse images of the formation of MCF-7 multicellular tumor spheroids on 100 μm micropatterns. This material is available free of charge via the Internet at http://pubs.acs.org.

■ AUTHOR INFORMATION

Corresponding Author

*E-mail: Benjamin.Thierry@unisa.edu.au.

Notes

The authors declare no competing financial interest.

■ ACKNOWLEDGMENTS

This work was supported by the NH&MRC Project Grant APP1045841. This work was performed, in part, at the South Australian node of the Australian National Fabrication Facility, a company established under the National Collaborative Research Infrastructure Strategy to provide nano- and micro-fabrication facilities for Australia's researchers. The authors acknowledge the facilities and scientific and technical assistance of the Australian Microscopy & Microanalysis Research Facility at the South Australian Regional Facility, University of South Australia, a facility that is funded by the University and State and Federal Governments.

■ REFERENCES

(1) Page, H.; Flood, P.; Reynaud, E. G. Three-Dimensional Tissue Cultures: Current Trends and Beyond. *Cell Tissue Res.* **2013**, *352*, 123−131.

(2) Hirschhaeuser, F.; Menne, H.; Dittfeld, C.; West, J.; Mueller-Klieser, W.; Kunz-Schughart, L. A. Multicellular Tumor Spheroids: an Underestimated Tool is Catching Up Again. *J. Biotechnol.* **2010**, *148*, 3−15.

(3) Hutmacher, D. Biomaterials Offer Cancer Research the Third Dimension. *Nat. Mater.* **2010**, *9*, 90−93.

(4) Peck, Y.; Wang, D.-A. Three-Dimensionally Engineered Biomimetic Tissue Models for *In Vitro* Drug Evaluation: Delivery, Efficacy and Toxicity. *Expert Opin. Drug Delivery* **2013**, *10*, 369−383.

(5) Kimlin, L.; Kassis, J.; Virador, V. 3D *In Vitro* Tissue Models and Their Potential for Drug Screening. *Expert Opin. Drug Delivery* **2013**, *8*, 1455−1466.

(6) Breslin, S.; O'Driscoll, L. Three-Dimensional Cell Culture: the Missing Link in Drug Discovery. *Drug Discovery Today* **2013**, *18*, 240−249.

(7) Kimlin, L. C.; Casagrande, G.; Virador, V. M. *In Vitro* Three-Dimensional (3D) Models in Cancer Research: An Update. *Mol. Carcinog.* **2013**, *52*, 167−182.

(8) Tung, Y.-C.; Hsiao, A. Y.; Allen, S. G.; Torisawa, Y.-s.; Ho, M.; Takayama, S. High-Throughput 3D Spheroid Culture and Drug Testing using a 384 Hanging Drop Array. *Analyst* **2011**, *136*, 473−478.

(9) Zorlutuna, P.; Annabi, N.; Camci-Unal, G.; Nikkhah, M.; Cha, J. M.; Nichol, J. W.; Manbachi, A.; Bae, H.; Chen, S.; Khademhosseini, A. Microfabricated Biomaterials for Engineering 3D Tissues. *Adv. Mater.* **2012**, *24*, 1782−1804.

(10) Charnley, M.; Textor, M.; Khademhosseini, A.; Lutolf, M. Integration Column: Microwell Arrays for Mammalian Cell Culture. *Integr. Biol.* **2009**, *1*, 625−634.

(11) Mehta, G.; Hsiao, A. Y.; Ingram, M.; Luker, G. D.; Takayama, S. Opportunities and Challenges for Use of Tumor Spheroids as Models to Test Drug Delivery and Efficacy. *J. Controlled Release* **2012**, *164*, 192−204.
(12) Kim, C.; Bang, J. H.; Kim, Y. E.; Lee, S. H.; Kang, J. Y. On-chip Anticancer Drug Test of Regular Tumor Spheroids Formed in Microwells by a Distributive Microchannel Network. *Lab Chip* **2012**, *12*, 4135−4142.
(13) Li, X.; Zhang, X.; Zhao, S.; Wang, J.; Liu, G.; Du, Y. Micro-Scaffold Array Chip for Upgrading Cell-based High-Throughput Drug Testing to 3D Using Benchtop Equipment. *Lab Chip* **2014**, *14*, 471−481.
(14) Otsuka, H.; Hirano, A.; Nagasaki, Y.; Okano, T.; Horiike, Y.; Kataoka, K. Two-Dimensional Multiarray Formation of Hepatocyte Spheroids on a Microfabricated PEG-Brush Surface. *ChemBioChem* **2004**, *5*, 850−855.
(15) Wang, W.; Itaka, K.; Ohba, S.; Nishiyama, N.; Chung, U.; Yamasaki, Y.; Kataoka, K. 3D Spheroid Culture System on Micropatterned Substrates for Improved Differentiation Efficiency of Multipotent Mesenchymal Stem Cells. *Biomaterials* **2009**, *30*, 2705−2715.
(16) Tamura, T.; Sakai, Y.; Nakazawa, K. Two-Dimensional Microarray of HepG2 Spheroids Using Collagen/Polyethylene Glycol Micropatterned Chip. *J. Mater. Sci., Mater. Med.* **2008**, *19*, 2071−2077.
(17) Kojima, R.; Yoshimoto, K.; Takahashi, E.; Ichino, M.; Miyoshi, H.; Nagasaki, Y. Spheroid Array of Fetal Mouse Liver Cells Constructed on a PEG−Gel Micropatterned Surface: Upregulation of Hepatic Functions by Co-Culture with Nonparenchymal Liver Cells. *Lab Chip* **2009**, *9*, 1991−1993.
(18) Hardelauf, H.; Frimat, J.-P.; Stewart, J. D.; Schormann, W.; Chiang, Y.-Y.; Lampen, P.; Franzke, J.; Hengstler, J. G.; Cadenas, C.; Kunz-Schughart, L. A.; West, J. Microarrays for the Scalable Production of Metabolically Relevant Tumour Spheroids: a Tool for Modulating Chemosensitivity Traits. *Lab Chip* **2011**, *11*, 419−428.
(19) Otsuka, H.; Sasaki, K.; Okimura, S.; Nagamura, M.; Nakasone, Y. Micropatterned Co-Culture of Hepatocyte Spheroids Layered on Non-Parenchymal Cells to Understand Heterotypic Cellular Interactions. *Sci. Technol. Adv. Mater.* **2013**, *14*, 065003.
(20) Lehnert, D.; Wehrle-Haller, B.; David, C.; Weiland, U.; Ballestrem, C.; Imhof, B. A.; Bastmeyer, M. Cell Behaviour on Micropatterned Substrata: Limits of Extracellular Matrix Geometry for Spreading and Adhesion. *J. Cell Sci.* **2004**, *117*, 41−52.
(21) Roth, E. A.; Xu, T.; Das, M.; Gregory, C.; Hickman, J. J.; Boland, T. Inkjet Printing for High-Throughput Cell Patterning. *Biomaterials* **2004**, *25*, 3707−3715.
(22) Agasti, S. S.; Chompoosor, A.; You, C.-C.; Ghosh, P.; Kim, C. K.; Rotello, V. M. Photoregulated Release of Caged Anticancer Drugs from Gold Nanoparticles. *J. Am. Chem. Soc.* **2009**, *131*, 5728−5729.
(23) Otsuka, H. Nanofabrication of Nonfouling Surfaces for Micropatterning of Cell and Microtissue. *Molecules* **2010**, *15*, 5525−5546.
(24) Hwang, I.-T.; Jung, C.-H.; Choi, J.-H.; Nho, Y.-C. Simple and Biocompatible Micropatterning of Multiple Cell Types on a Polymer Substrate by Using Ion Implantation. *Langmuir* **2010**, *26*, 18437−18441.
(25) Takano, T.; Yamaguchi, S.; Matsunuma, E.; Komiya, S.; Shinkai, M.; Takezawa, T.; Nagamune, T. Cell Transfer Printing from Patterned Poly(Ethylene Glycol)−Oleyl Surfaces to Biological Hydrogels for Rapid and Efficient Cell Micropatterning. *Biotechnol. Bioeng.* **2012**, *109*, 244−251.
(26) Siow, K. S.; Britcher, L.; Kumar, S.; Griesser, H. J. Plasma Methods for the Generation of Chemically Reactive Surfaces for Biomolecule Immobilization and Cell Colonization—A Review. *Plasma Process. Polym.* **2006**, *3*, 392−418.
(27) Muguruma, H. Plasma-Polymerized Films for Biochip Design. *Plasma Process. Polym.* **2010**, *7*, 151−162.
(28) Yang, Z.; Tu, Q.; Wang, J.; Lei, X.; He, T.; Sun, H.; Huang, N. Bioactive Plasma-Polymerized Bipolar Films for Enhanced Endothelial Cell Mobility. *Macromol. Biosci.* **2011**, *11*, 797−805.
(29) Hamerli, P.; Weigel, T.; Groth, T.; Paul, D. Surface Properties of and Cell Adhesion onto Allylamine-Plasma-Coated Polyethylenterephtalat Membranes. *Biomaterials* **2003**, *24*, 3989−3999.
(30) Finke, B.; Luethen, F.; Schroeder, K.; Mueller, P. D.; Bergemann, C.; Frant, M.; Ohl, A.; Nebe, B. J. The Effect of Positively Charged Plasma Polymerization on Initial Osteoblastic Focal Adhesion on Titanium Surfaces. *Biomaterials* **2007**, *28*, 4521−4534.
(31) Thissen, H.; Johnson, G.; Hartley, P. G.; Kingshott, P.; Griesser, H. J. Two-Dimensional Patterning of Thin Coatings for the Control of Tissue Outgrowth. *Biomaterials* **2006**, *27*, 35−43.
(32) Punzon-Quijorna, E.; Sanchez-Vaquero, V.; Noval, A. M.; Perez, D. G.; Font, A. C.; Ceccone, G.; Gago, R.; Ruiz, J. P. G.; Silvan, M. M. Optimized Allylamine Deposition for Improved Pluripotential Cell Culture. *Vacuum* **2011**, *85*, 1071−1075.
(33) Testrich, H.; Rebl, H.; Finke, B.; Hempel, F.; Nebe, B.; Meichsner, J. Aging Effects of Plasma Polymerized Ethylenediamine (PPEDA) Thin Films on Cell-Adhesive Implant Coatings. *Mater. Sci. Eng., C* **2013**, *33*, 3875−3880.
(34) Cheng, Q.; Komvopoulos, K.; Li, S. Surface Chemical Patterning for Long-Term Single-Cell Culture. *J. Biomed. Mater. Res., Part A* **2011**, *96A*, 507−512.
(35) Bouaidat, S.; Berendsen, C.; Thomsen, P.; Petersen, S. G.; Wolff, A.; Jonsmann, J. Micro patterning of Cell and Protein Non-Adhesive Plasma Polymerized Coatings for Biochip Applications. *Lab Chip* **2004**, *4*, 632−637.
(36) Cheng, Q.; Li, S.; Komvopoulos, K. Plasma-Assisted Surface Chemical Patterning for Single-Cell Culture. *Biomaterials* **2009**, *30*, 4203−4210.
(37) Cheng, Q.; Komvopoulos, K. Integration of Plasma-Assisted Surface Chemical Modification, Soft Lithography, and Protein Surface Activation for Single-Cell Patterning. *Appl. Phys. Lett.* **2010**, *97*, 043705.
(38) Dai, L.; Griesser, H. J.; Mau, A. W. H. Surface Modification by Plasma Etching and Plasma Patterning. *J. Phys. Chem. B* **1997**, *101*, 9548−9554.
(39) Jackman, R. J.; Duffy, D. C.; Cherniavskaya, O.; Whitesides, G. M. Using Elastomeric Membranes as Dry Resists and for Dry Lift-Off. *Langmuir* **1999**, *15*, 2973−2984.
(40) Thierry, B.; Jasieniak, M.; de Smet, L. C. P. M.; Vasilev, K.; Griesser, H. J. Reactive Epoxy-Functionalized Thin Films by a Pulsed Plasma Polymerization Process. *Langmuir* **2008**, *24*, 10187−10195.
(41) Liu, T.; Thierry, B. A Solution to the PEG Dilemma: Efficient Bioconjugation of Large Gold Nanoparticles for Biodiagnostic Applications using Mixed Layers. *Langmuir* **2012**, *28*, 15634−15642.
(42) Liu, T.; Cousins, A.; Chien, C.-C.; Kempson, I.; Thompson, S.; Hwu, Y.; Thierry, B. Immunospecific Targeting of CD45 Expressing Lymphoid Cells: Towards Improved Detection Agents of the Sentinel Lymph Node. *Cancer Lett.* **2013**, *328*, 271−277.
(43) Nejadnik, M. R.; Olsson, A. L. J.; Sharma, P. K.; van der Mei, H. C.; Norde, W.; Busscher, H. J. Adsorption of Pluronic F-127 on Surfaces with Different Hydrophobicities Probed by Quartz Crystal Microbalance with Dissipation. *Langmuir* **2009**, *25*, 6245−6249.
(44) Schroen, C. G. P. H.; Stuart, M. A. C.; van der Voort Maarschalk, K.; van der Padt, A.; van't Riet, K. Influence of Preadsorbed Block Copolymers on Protein Adsorption: Surface Properties, Layer Thickness, and Surface Coverage. *Langmuir* **1995**, *11*, 3068−3074.
(45) Bullett, N. A.; Short, R. D.; O'Leary, T.; Beck, A. J.; Douglas, C. W. I.; Cambray-Deakin, M.; Fletcher, I. W.; Roberts, A.; Blomfield, C. Direct Imaging of Plasma-Polymerized Chemical Micropatterns. *Surf. Interface Anal.* **2001**, *31*, 1074−1076.
(46) Szili, E.; Thissen, H.; Hayes, J. P.; Voelcker, N. A Biochip Platform for Cell Transfection Assays. *Biosens. Bioelectron.* **2004**, *19*, 1395−1400.
(47) Liu, V. A.; Jastromb, W. E.; Bhatia, S. N. Engineering Protein and Cell Adhesivity Using PEO-Terminated Triblock Polymers. *J. Biomed. Mater. Res.* **2002**, *60*, 126−134.
(48) Wu, M.-H. Simple Poly(dimethylsiloxane) Surface Modification to Control Cell Adhesion. *Surf. Interface Anal.* **2009**, *41*, 11−16.

(49) Klein, S.; Petersen, S.; Taylor, U.; Rath, D.; Barcikowski, S. Quantitative Visualization of Colloidal and Intracellular Gold Nanoparticles by Confocal Microscopy. *J. Biomed. Opt.* **2010**, *15*, 036015.
(50) Taylor, U.; Klein, S.; Petersen, S.; Kues, W.; Barcikowski, S.; Rath, D. Nonendosomal Cellular Uptake of Ligand-Free, Positively Charged Gold Nanoparticles. *Cytometry A* **2010**, *77A*, 439−446.
(51) Davis, M. E. The First Targeted Delivery of siRNA in Humans via a Self-Assembling, Cyclodextrin Polymer-Based Nanoparticle: From Concept to Clinic. *Mol. Pharm.* **2009**, *6*, 659−668.
(52) Davis, M. E.; Zuckerman, J. E.; Choi, C. H. J.; Seligson, D.; Tolcher, A.; Alabi, C. A.; Yen, Y.; Heidel, J. D.; Ribas, A. Evidence of RNAi in Humans from Systemically Administered siRNA via Targeted Nanoparticles. *Nature* **2010**, *464*, 1067−1070.